

Selective Growth of Vertical-aligned ZnO Nanorod Arrays on Si Substrate by Catalyst-free Thermal Evaporation

H. Wang · Z. P. Zhang · X. N. Wang ·
Q. Mo · Y. Wang · J. H. Zhu · H. B. Wang ·
F. J. Yang · Y. Jiang

Received: 3 July 2008 / Accepted: 5 August 2008 / Published online: 21 August 2008
© to the authors 2008

Abstract By thermal evaporation of pure ZnO powders, high-density vertical-aligned ZnO nanorod arrays with diameter ranged in 80–250 nm were successfully synthesized on Si substrates covered with ZnO seed layers. It was revealed that the morphology, orientation, crystal, and optical quality of the ZnO nanorod arrays highly depend on the crystal quality of ZnO seed layers, which was confirmed by the characterizations of field-emission scanning electron microscopy, X-ray diffraction, transmission electron microscopy, and photoluminescence measurements. For ZnO seed layer with wurtzite structure, the ZnO nanorods grew exactly normal to the substrate with perfect wurtzite structure, strong near-band-edge emission, and neglectable deep-level emission. The nanorods synthesized on the polycrystalline ZnO seed layer presented random orientation, wide diameter, and weak deep-level emission. This article provides a C-free and Au-free method for large-scale synthesis of vertical-aligned ZnO nanorod arrays by controlling the crystal quality of the seed layer.

Keywords ZnO · Thermal evaporation · Nanorod arrays · Seed layer · Catalyst-free

Introduction

In the recent years, quasi-one-dimensional (1D) ZnO nanostructures such as nanopores, [1] nanowires, [2] nanobelts [3], and nanorods [4] have attracted great interest due to their unique electrical and photonic properties for potential applications in chemical sensors, optoelectronics, and field-effect transistors. Thanks to the high surface-volume ratio, controllability of the nucleation position, and superior ultraviolet lasing and photoluminescence (PL) property of ZnO nanorods or nanoarrays [5–7], the realization of vertically well-aligned 1D ZnO nanorods is very important for its application in nanoscale light-emitting diodes (LEDs), nanosensors, and field emitters [8–11]. In order to fabricate ZnO nanorods, various methods including thermal evaporation [12–15], chemical vapor deposition [16], metal organic chemical vapor deposition (MOCVD) [17, 18], and solution-based methods have been used [19]. Among the numerous researches on the synthesis and properties of ZnO nanorods, uniform ZnO nanorod arrays have been successfully prepared on sapphire substrates by Au-catalyzed vapor–liquid–solid (VLS) growth with or without the use of GaN template [5, 20]. However, Au impurities will be unavoidably left on the tip of the nanorods after the growth [21], which is detrimental to device performance. In addition, the insulating and expensive sapphire substrate is also disadvantageous for the integration of nanorod arrays with the current primary stream of the Si-based device technology. At the same time, using ZnO film as seed layer, vertical-aligned ZnO nanorods have been grown on silicon substrate by thermal evaporation of ZnO–C powder mixture [13–15]. Since the type of such nanorods growth is dominated by the carbothermal reduction of ZnO–C powder mixture [15], the introduction of C atoms will possibly bring adverse effect on nanorods

H. Wang · Z. P. Zhang · X. N. Wang (✉) · Q. Mo · Y. Wang ·
J. H. Zhu · H. B. Wang · F. J. Yang
Faculty of Physics and Electronic Technology, Hubei University,
Wuhan 430062, People's Republic of China
e-mail: xnwang2006@hotmail.com

Y. Jiang
School of Materials Science and Engineering, University of
Science and Technology Beijing, Beijing 100083, China

application in device integration. Furthermore, this type of nanorods growth usually needs a relatively high ramp rate of furnace temperature (e.g., 25 °C/min) to obtain a high Zn saturation pressure [13], and even much higher ramp rate (e.g., 75 °C/min) has to be satisfied in order to increase the spacing between the nanorods [15]. It is well known that there is a big difference in the thermal expansion coefficients as well as the big lattice mismatch between Si ($2.56 \times 10^{-6} \text{ K}^{-1}$) and ZnO ($4.75 \times 10^{-6} \text{ K}^{-1}$) [22], such high ramp rate is not good for the relaxation of the thermal strain in the underlying ZnO film, which can accelerate the generation of structure defects or even cracks [23], and then greatly affects the properties of the upper nanorods. Therefore, new techniques are required in order to obtain vertical-aligned ZnO nanorods on Si substrate. On the other hand, although ZnO seed layer is very important for the nucleation and growth of ZnO nanorods or nanoarrays [19, 24–26], there is very little literature about the influence of ZnO seed layer quality on the orientation, morphology, crystal, and optical quality of the upper ZnO nanorods grown by thermal evaporation method.

In this article, a catalyst and carbon-free evaporation method was demonstrated to synthesize high-density well-aligned ZnO nanorod arrays on Si(100) substrates pre-deposited by ZnO seed layers with different crystal quality and morphology. A low rate was adopted during the ramping and cooling of the furnace considering the large difference in the thermal expansion coefficient of Si and ZnO. It was found that the nanorod arrays grown on the ZnO films with better crystal quality have vertical orientation as well as better optical and crystal quality. This method not only provides a very easy way for the large-scale synthesis of nanorod arrays on semiconductor substrates, but also avoids the introduction of the impurities caused by metal catalysts or carbon.

Experimental Details

Two ZnO film templates (a and b) were prepared by RF sputtering and pulsed laser deposition (PLD) on Si(100) substrates for the deposition of ZnO nanorod arrays, respectively. High-purity ZnO powder (4 N) was put into an alumina crucible placed at the center of an alumina tube furnace ($\Phi 6.0 \times 100 \text{ cm}$). The ZnO/Si(100) substrates were placed at 24 cm away from the evaporation source in the alumina tube. After being purged by high-purity Ar for 30 min, the furnace temperature was raised to 800 °C with a rate of 10 °C/min under a constant Ar flow of 60 sccm. After the furnace was maintained at 800 °C for 30 min, it was heated to 1,400 °C within 120 min and maintained at 1,400 °C for the evaporation of ZnO onto prior ZnO/Si template for 90 min, during which the pressure was kept

within 0.025–0.03 MPa. Then the furnace was cooled down with a rate of 5 °C/min. The substrates were taken out the furnace after it was cooled down to room temperature, and a white wax-like layer can be clearly seen deposited onto the substrates.

The morphology and crystal quality of the ZnO nanorod arrays and the pre-deposited ZnO films were investigated by field-emission scanning electron microscopy (FE-SEM, JEOL JSM-6700F) and X-ray diffraction (XRD, Brukers D8) measurements. Further microstructure information was studied by a high-resolution transmission electron microscopy (HRTEM, Tecnai G20). The optical property of the ZnO nanorod arrays was examined by PL measurements executed at room temperature using He–Cd laser (325 nm) as excitation source.

Results and Discussion

Figure 1a shows the cross-sectional FE-SEM images of the ZnO nanorod arrays synthesized on ZnO films prepared by RF sputtering. It can be clearly seen that most of the nanorods grow upward with various angles $<45^\circ$ off the normal direction of the substrate surface with a uniform height and diameter of about 5.5 and 1.5 μm , respectively. It is very strange that several nanorods lie on the substrate very randomly. To judge whether the fallen nanorods is due to SEM sample preparation, an SEM analysis was done from a top view (as shown by the inset) which avoids possible destruction by foreign force used in the sample preparation. As shown in the inset picture, the nanorods stand on the substrates instead of lying on the substrate, which indicates that the fallen nanorods shown in Fig. 1a are likely to be caused by the SEM sample preparation. Moreover, the nanorods crystal has a typical prismatic shape with pencil-like end top. Figure 1b and the inset show the cross-sectional FE-SEM images and an enlarged view of the ZnO nanorod arrays synthesized on ZnO films prepared by PLD, respectively. High-density ZnO nanorod arrays can be observed exactly along the normal direction of the substrate surface. In addition, the length and diameter of the ZnO nanorods are in the range of 2–4 μm and 80–250 nm, respectively, and the average diameter is about 150 nm. Comparing the above two types of ZnO nanorods, it is obviously that the nanorod arrays grown on the ZnO film prepared by PLD have better vertical orientation and much smaller average rod diameter than those on the ZnO film prepared by RF sputtering.

Figure 2a and b shows the XRD results of the nanorods synthesized on the two films. For the ZnO nanorods on the ZnO film prepared by RF sputtering, besides the sharp ZnO (0002) diffraction peak around 34.41° , ZnO (10 $\bar{1}$ 1), (10 $\bar{1}$ 2), (10 $\bar{1}$ 3) diffraction peaks can also be detected.

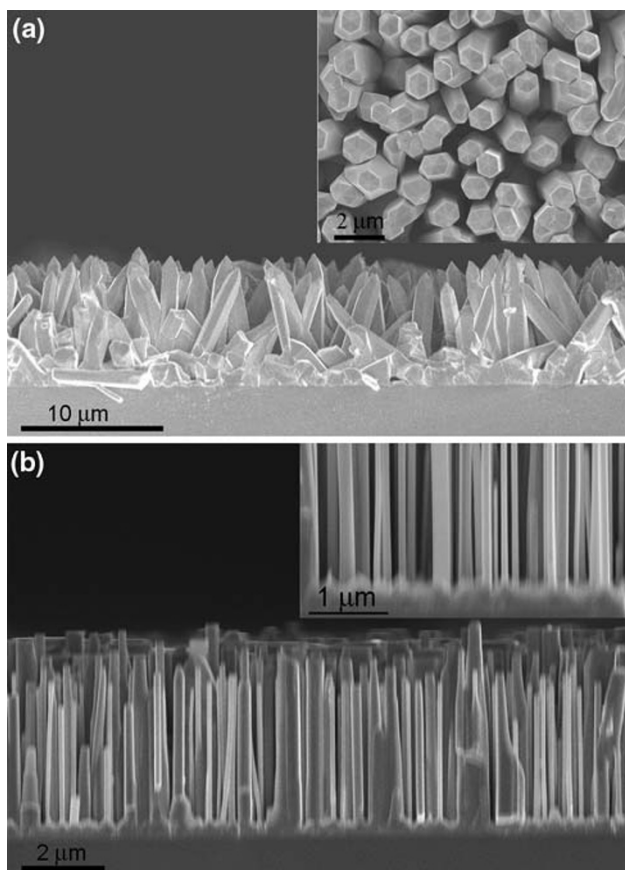


Fig. 1 Cross-sectional FE-SEM images of ZnO nanorods synthesized on the ZnO films prepared by RF sputtering (a) and PLD (b), respectively. The inset in (a) shows the top view of the corresponding sample, the inset in (b) is the corresponding enlarged image

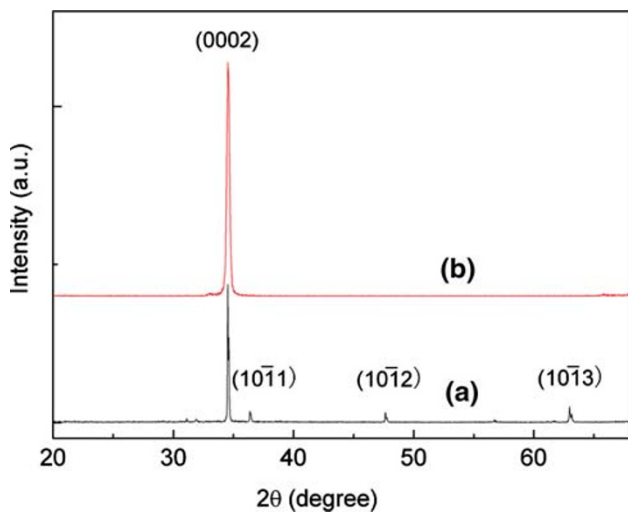


Fig. 2 θ - 2θ XRD patterns of the as-prepared well-aligned ZnO nanorods on the ZnO film prepared by RF sputtering (a) and PLD (b), respectively

While only a sharp ZnO (0002) diffraction peak can be observed in Fig. 2b, its suggesting that the nanorods have a pure wurtzite structure, which also indicates that the degree

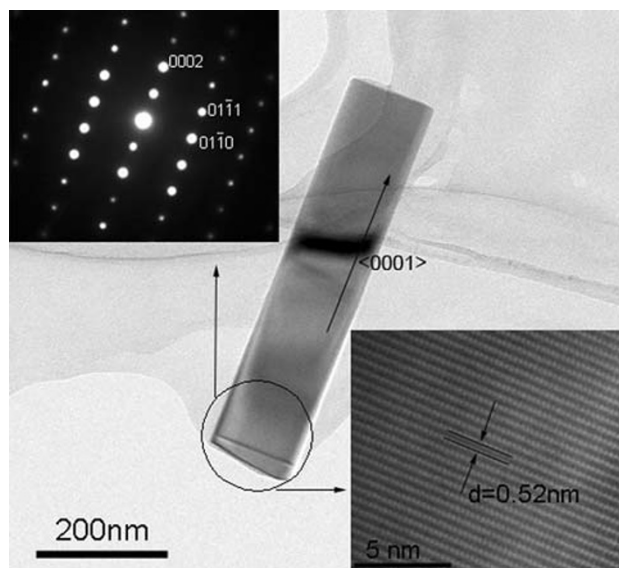


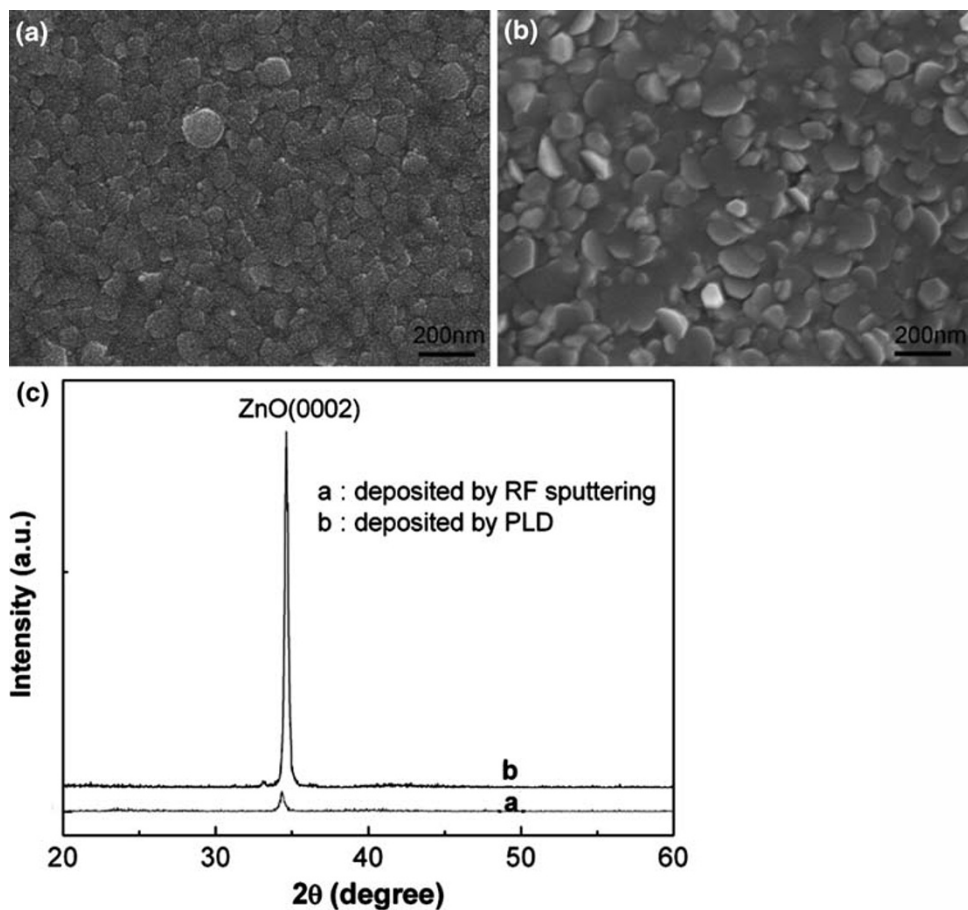
Fig. 3 LR-TEM image of one nanorod synthesized on the ZnO film prepared by PLD. Insets show the corresponding HRTEM image and SAED pattern taken from the circled area in the ZnO nanorod with the incident direction of electrons paralleling the cross-section of the nanorod

of orientation of the nanorods on the film prepared by PLD is much higher than those on the film prepared by RF sputtering. As the nanorods in Fig. 1b grown along the normal direction of the substrate surface, the XRD result strongly suggests that the growth direction of the nanorods on the ZnO films prepared by PLD is along ZnO [0001]. Moreover, since neither catalysts nor carbon were used in our synthesis process, no impurity was detected in the XRD measurement.

More detailed structure of the ZnO nanorod on the ZnO seed layer prepared by PLD was further investigated using TEM. Figure 3 shows a low-resolution (LR-TEM) image, HRTEM image, and selected area electron diffraction (SAED) pattern of a single ZnO nanorod, which was washed off from the as-prepared product. It is clear that the ZnO nanorod is very straight with an extremely uniform diameter of about 150 nm in accordance to the FE-SEM observation. Both the SAED pattern and HRTEM picture strongly suggest that the nanorod has a single-domain wurtzite structure with high crystal quality. The HRTEM picture also shows that the lattice distance along the arrow is about 0.52 nm, well consistent with that along *c*-axis of bulk wurtzite ZnO crystal [27]. As the SAED pattern and HRTEM picture were taken from the circled area in the ZnO nanorod, and the incidence angle of high electrons was adopted along the cross-section of the nanorod, it can be concluded that the nanorod grows exactly along the ZnO [0001] direction, and well consistent with the above XRD result.

In order to study the role the ZnO seed layer played in selective growth of ZnO nanorods, a morphology and

Fig. 4 FE-SEM images of ZnO seed layers deposited by RF sputtering (a) and PLD (b), respectively. (c) Shows the θ - 2θ XRD patterns of the corresponding ZnO seed layers



crystal characterization were performed on the ZnO seed layer. Figure 4a and b shows the FE-SEM images of the seed layers prepared by RF sputtering (a) and PLD (b), respectively. Both films have small grains with a diameter ranged from several tens to hundreds nanometer. Figure 4c shows the θ - 2θ XRD patterns of the seed layers. A sharp diffraction peak can be clearly seen at 34.64° for seed layer (b), suggesting the ZnO film prepared by PLD has good crystal quality with a wurtzite structure. Compared with (b), the crystal quality of film (a) is very poor with a very weak diffraction peak. Since both the ZnO nanorods samples were prepared under the same condition in the furnace including the source temperature, the distance between source and substrate and Ar flow; it can be concluded that the crystal quality is a key factor influencing the orientation and the crystal quality of the above ZnO nanorod arrays.

Based on the above property of the seed layers and nanorod samples, a possible growth mechanism for ZnO nanorods was proposed. It has long been held that ZnO nanorods always nucleate from the concave tip near the grain boundary between two ZnO film grains [26], the high-density small grains shown in Fig. 4a and b naturally provide numerous nucleation sites for ZnO growth. For the seed layer with good wurtzite structure, ZnO will adopt the

same epitaxial relationship as the seed layer. At the same time, the lateral growth of ZnO is greatly limited while the growth along [0001] direction dominates the whole growth process considering the different growth rate of various growth facets which followed in the order of $[0001] > [10\bar{1}1] > [10\bar{1}0]$ [28]. Therefore, well vertical-aligned ZnO nanorods will be obtained on the ZnO template prepared by PLD. As for the template with poor crystal quality, though the preferential growth direction is along [0001] ZnO azimuth, the orientation of the nanorods will be very disordered relative to the substrate at the initial stage because of the randomly distributed grains in the ZnO seed layer. With growth time increasing, adjacent nanorods tend to coalesce into a wider nanorod with larger diameter once these thinner nanorods meet each other at side faces. Thus, though there is no obvious difference between the grain sizes of the two types of the seed layer, the diameter of the nanorods growing on them varies to a great degree. Therefore, the orientation and the diameter of the nanorods are highly dependent on the crystal quality of the underlying ZnO seed layer.

The optical quality of the two types of ZnO nanorods was investigated by PL measurement performed at room temperature using He-Cd laser as excitation source with

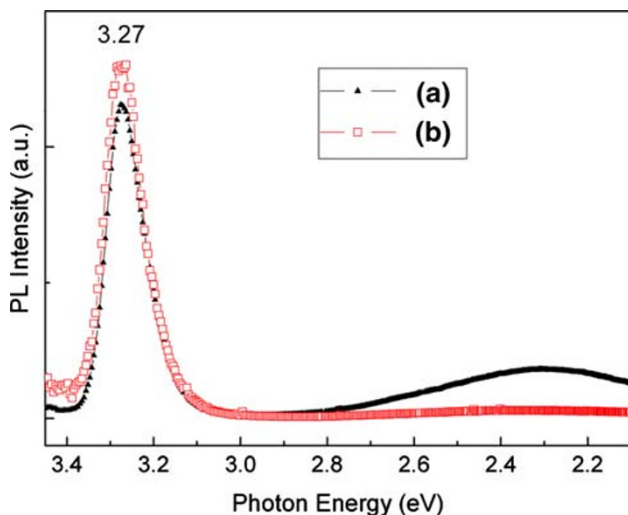


Fig. 5 Room-temperature PL spectra of the nanorod arrays on the ZnO films prepared by RF sputtering (a) and PLD (b), respectively

wavelength of 325 nm. Figure 5 shows the result of PL spectra. For the ZnO nanorods with disordered orientation, a sharp and strong near-band-edge (NBE) emission can be clearly found at about 3.27 eV attributed to the direct recombination of free excitons from the ZnO nanorod arrays [29], and a weak emission band occurs in the range of 2.6 to 2.1 eV. As previous literature reports, the green emission is related to the singly ionized oxygen vacancy and the recombination of a photo-generated hole with a singly ionized charge state of the specific defects [30, 31]. The intensity of NBE emission is enhanced for the ZnO nanorods with good vertical orientation, while the deep-level emission in the lower energy side caused by the defect has been greatly decreased. The high optical quality of the nanorods arrays can be attributed to good crystal quality and the well-orientation growth, well consistent with the above XRD results. The results also indicate the superiority of our method using pure ZnO powder as evaporation source without the introduction of C or Au.

Conclusion

In conclusion, vertically well-aligned 1D ZnO nanorod arrays with high quality have been achieved without any catalyst or C on the ZnO seed layers prepared by PLD. The dependence of the orientation, morphology, crystal quality, and optical quality of the nanorod arrays on the quality of the seed layer is systematically studied by FE-SEM, XRD, HRTEM, and PL analysis. It is found that for the ZnO seed layer with good crystal quality, the nanorods grow exactly along ZnO [0001] direction with perfect wurtzite structure, small diameter (150 nm), and high optical quality. While for the ZnO seed layer with poor crystal quality, the nanorods

grow in random directions with weak deep-level emission and wider diameter (about 1.5 μm). This article not only provides an easy and clean way to fabricate large-scale well-aligned ZnO nanorods, but also sheds light on controlling the orientation, diameter, and quality of ZnO nanorods by increasing the crystal quality of ZnO seed layer.

Acknowledgments This work is supported in part by the National Nature Science Foundation of China (No.50772032), MOST of China (No.2007CB936202), Research Fund for the Doctoral Program of China Education Ministry (20060512004), Natural Science Foundation Creative Team Project of Hubei Province (2007ABC005).

References

- G.Q. Ding, W.Z. Shen, M.J. Zheng, D.H. Fan, *Appl. Phys. Lett.* **88**, 103106 (2006). doi:10.1063/1.2182025
- M.H. Huang, S. Mao, H. Feick, H. Yan, Y. Wu, H. Kind et al., *Science* **292**, 1897 (2001). doi:10.1126/science.1060367
- Z.W. Pan, Z.R. Dai, Z.L. Wang, *Science* **291**, 1947 (2001). doi:10.1126/science.1058120
- J.Y. Li, X.L. Chen, H. Li, M. He, Z.Y. Qiao, *J. Cryst. Growth* **233**, 5 (2001). doi:10.1016/S0022-0248(01)01509-3
- D.F. Liu, Y.J. Xiang, Q. Liao, J.P. Zhang, X.C. Wu, Z.X. Zhang et al., *Nanotechnology* **18**, 405303 (2007). doi:10.1088/0957-4484/18/40/405303
- X.H. Han, G.Z. Wang, Q.T. Wang, L. Cao, R.B. Liu, B.S. Zou et al., *Appl. Phys. Lett.* **86**, 223106 (2005). doi:10.1063/1.1941477
- C. Li, G.J. Fang, F.H. Su, G.H. Li, X.G. Wu, X.Z. Zhao, *Nanotechnology* **17**, 3740 (2006). doi:10.1088/0957-4484/17/15/021
- A. Yoon, W.-K. Hong, T. Lee, *J. Nanosci. Nanotechnol.* **7**, 4101 (2007). doi:10.1166/jnn.2007.011
- W.I. Park, G.-C. Yi, *Adv. Mater.* **16**, 87 (2004). doi:10.1002/adma.200305729
- M.S. Arnold, P. Avouris, Z.W. Pan, Z.L. Wang, *J. Phys. Chem. Br.* **107**, 659 (2003)
- S.Y. Li, P. Lin, C.Y. Lee, T.Y. Tseng, *J. Appl. Phys.* **95**, 3711 (2004). doi:10.1063/1.1655685
- A.K. Pradhan, T.M. Williams, K. Zhang, D. Hunter, J.B. Dadson, K. Lord et al., *J. Nanosci. Nanotechnol.* **6**, 1985 (2006). doi:10.1166/jnn.2006.318
- C. Li, G.J. Fang, N.S. Liu, J. Li, L. Liao, F.H. Su et al., *J. Phys. Chem. C* **111**, 12566 (2007). doi:10.1021/jp0737808
- J.S. Jie, G.Z. Wang, Y.M. Chen, X.H. Han, Q.T. Wang, B. Xu et al., *Appl. Phys. Lett.* **86**, 031909 (2005). doi:10.1063/1.1854737
- R.T.R. Kumar, E. McGlynn, C. McLoughlin, S. Chakrabarti, R.C. Smith, J.D. Carey et al., *Nanotechnology* **18**, 215704 (2007). doi:10.1088/0957-4484/18/21/215704
- Y. Liu, M. Liu, *J. Nanosci. Nanotechnol.* **7**, 4529 (2007). doi:10.1166/jnn.2007.874
- S.H. Park, S.W. Han, *J. Nanosci. Nanotechnol.* **7**, 2909 (2007). doi:10.1166/jnn.2007.604
- G.W. Cong, H.Y. Wei, P.F. Zhang, W.Q. Peng, J.J. Wu, X.L. Liu et al., *Appl. Phys. Lett.* **87**, 231903 (2005). doi:10.1063/1.2137308
- Y.-J. Kim, C.-H. Lee, Y. Joon, G.-C. Yi, S.S. Kim, H. Cheong, *Appl. Phys. Lett.* **89**, 163128 (2006). doi:10.1063/1.2364162
- H. Zhou, M. Wissinger, J. Fallert, R. Hauschild, F. Stelzl, C. Klingshirn et al., *Appl. Phys. Lett.* **91**, 181112 (2007). doi:10.1063/1.2805073

21. S. Kodambaka, J. Tersoff, M.C. Reuter, F.M. Ross, *Science* **316**, 729 (2007). doi:[10.1126/science.1139105](https://doi.org/10.1126/science.1139105)
22. O. Madelung, *Numerical Data and Functional Relationships in Science and Technology* (Springer, Heidelberg, 1982)
23. Y.F. Chen, F.Y. Jiang, L. Wang, C.D. Zheng, J.N. Dai, Y. Pu et al., *J. Cryst. Growth* **275**, 486 (2005). doi:[10.1016/j.jcrysgro.2004.12.019](https://doi.org/10.1016/j.jcrysgro.2004.12.019)
24. Q. Ahsanulhaq, J.-H. Kim, Y.-B. Hahn, *Nanotechnology* **18**, 485307 (2007). doi:[10.1088/0957-4484/18/48/485307](https://doi.org/10.1088/0957-4484/18/48/485307)
25. Q. Ahsanulhaq, A. Umar, Y.B. Hahn, *Nanotechnology* **18**, 115603 (2007). doi:[10.1088/0957-4484/18/11/115603](https://doi.org/10.1088/0957-4484/18/11/115603)
26. Y. Tak, D. Park, K. Yong, *J. Vac. Sci. Technol. B* **24**, 2047 (2006). doi:[10.1116/1.2216714](https://doi.org/10.1116/1.2216714)
27. Ü. Özgür, Y.I. Alivov, C. Liu, A. Teke, M.A. Reshchikov, S. Doğan et al., *J. Appl. Phys.* **98**, 041301 (2005). doi:[10.1063/1.1992666](https://doi.org/10.1063/1.1992666)
28. R.C. Wang, C.P. Liu, J.L. Huang, S.-J. Chen, *Appl. Phys. Lett.* **86**, 251104 (2005). doi:[10.1063/1.1948522](https://doi.org/10.1063/1.1948522)
29. V. Stikant, D.R. Clarke, *J. Appl. Phys.* **83**, 5447 (1998). doi:[10.1063/1.367375](https://doi.org/10.1063/1.367375)
30. J.Q. Hu, Y. Bando, *Appl. Phys. Lett.* **82**, 1401 (2003). doi:[10.1063/1.1558899](https://doi.org/10.1063/1.1558899)
31. Y. Li, G.S. Cheng, L.D. Zhang, *J. Mater. Res.* **15**, 2305 (2000). doi:[10.1557/JMR.2000.0331](https://doi.org/10.1557/JMR.2000.0331)